Chapter 8

Different Approaches of Synchronization in Chaotic-Coupled QD Lasers

Hussein B. Al Husseini and Kais A.M. Al Naimee

Additional information is available at the end of the chapter

http://dx.doi.org/10.5772/intechopen.72500

Abstract

The investigation of synchronization phenomena on measured theoretical data such as time series has recently become an increasing focus of interest. In this chapter, the synchronized states (including steady state, periodic or chaotic) in coupled quantum dot lasers (dimensionless rate equations) are considered with both bidirectional and unidirectional synchronization. Different approaches for measuring synchronization have been proposed that rely on certain characteristic features of the dynamical system under investigation. Results show that the measure to be applied to a certain task can be chosen according to information in test applications, although certain dynamical features of a system under investigation (e.g., bifurcation and amplitude correlation) may render certain measures more suitable than others.

Keywords: quantum-dot (QD) laser, optical feedback, bifurcation, dimensionless rate equations, chaos synchronization

1. Introduction

Idea of "exploit quantum effects in heterostructure semiconductor lasers to produce wavelength tunability" and achieve a "lower lasing threshold "via" the change in the density of states, which outcome from reducing the number of translational degrees of freedom of the carriers", was firstly introduced by Dingle and Henry in 1976 [1]. This is performed by reducing the thickness of the smaller band gap material (the active region) in the heterostructure to the scale of the deBroglie wavelength of the carrier (~ few nanometers). This results in a quantum well (QW) structure. Reducing the size of another dimension results in a quantum wire (QWi) structure. Further reduction of the remaining dimension results in a quantum dot (QD) structure where all dimensions are quantized. However, for about a quarter of century, lasers using structures with carrier confinement in two ("quantum wire") or all in

three ("quantum dot") directions appear to lack practical realization compared to so-called QW lasers, where quantum confinement of carriers occurs in one dimension.

The most important advantage of using size-quantized heterostructures in lasers originates from the increase in the density of states for charge carriers near band edges. When used as an active layer for the laser, this focuses most of the injected carriers in an increasingly narrow energy range near the bottom of the conduction band and/or the peak of the valence band. This enhances the maximum material gain (assuming the same homogeneous or inhomogeneous broadening as in bulk lasers) and reduces the influence of temperature on device performance making it less temperature dependent. This also makes further reduction in the threshold current. The electronic states in a QD are spatially localized and the energy is fully quantized, similar to a single atom [1]. So, the system is more stable against any thermal perturbation. In addition, due to the quantization, the probability becomes higher for optical transitions. Also, the electron localization may radically reduce the scattering of electrons by bulk defects and reduce the rate of non-radiative recombination. These properties, among the others, are directly related with the high thermal stability and the high quantum efficiency of QD lasers, and they are of great importance in terms of device applications.

From a dynamical behavior systems' point of view, semiconductor lasers are characterized by a time scale separation between the fast-slow systems, that is, fast photon and the slower carrier subsystem [2]. As a result, their turn-on dynamics shows damped nonlinear intensity oscillations, which are called relaxation oscillations. The damping of relaxation oscillations is a key point in order to understand the stability properties of the laser subject to external perturbations, for example, optical injection or optical feedback. QW laser shows obvious, weakly damped relaxation oscillations, while the relaxation oscillations of QD lasers are strongly damped [3]. As a result, QD lasers under optical injection display a higher dynamical stability [4] and optical feedback [5]. In QD devices, the carriers are first injected into a surrounding QW acting as a carrier reservoir, before they scatter into the discrete energy levels of the QDs, between which the optical transition takes place. The scattering rates of carrier strongly depend on the energy spacing between the band gap of the QW and the discrete QD levels, that is, on the band structure of the device. The scattering rates provide lifetimes of the nonlinear carriers in the QD levels, which yield additional time scales compared to QW lasers. The discrete energy levels determine how these time scales compare to the carrier lifetimes in the carrier reservoir and the photon lifetime. For a small energy spacing as example, short lifetimes (large scattering rates) are obtained, which are on the same time scale or shorter than the photon lifetime yielding over-damped, very stable system, which work similar to gas lasers, i.e., typical class A of lasers. For high level of energy, long carrier lifetimes are obtained, which guarantee an apparent time-scale separation between the carrier and the photon system (time-scale of femtoseconds) resulting in weakly damped, less stable lasers, whose dynamics is similar to conventional QW lasers, that is, typical class B lasers. QD lasers dynamics lie between these two limiting cases and show typical dynamical features of class B and class A lasers [3].

A characteristic of semiconductor lasers is its high sensitivity to external optical disturbances due to the relatively low reflection of its facets [4]. On the one hand, this may be a disadvantage,

because in optical applications, expensive isolators are needed to ensure a stable constant wave (CW) emission of lasers. Conversely, the basic physics of the views, the laser semiconductor display, subject to optical injection or optical feedback, a wealth of different dynamic systems ranging from stable cw emissions, with period behavior intensity modulations, to chaotic behavior [5].

Numerous applications arise from optical injection ranging from noise reduction [6], over a reduction of relative intensity noise [7], the strengthening side-mode suppression [8], to a larger bandwidth under direct optical alteration [9], and the generation of microwave signals [10].

Furthermore, the semiconductor lasers subject to delayed optical feedback are the ideal candidates to study the stabilization of steady states and limit cyclical orbits due to the control of nongaseous delayed feedback [10].

Moreover, delay synchronization of coupled lasers, bubbling in coupled lasers, and networks of delay coupled lasers [11] are subject of current research.

2. Nonlinear dynamics of QD

Currently, nonlinear laser dynamics is a field that continues to grow from active research, and this chapter focuses and reviews recent developments in this area with the approach of a new dimensional model. In a multipronged approach, it will also focus on mathematical and physical aspects. By discussing problems such as exploiting the chaotic laser for secure communications, using the QD laser applications, it will introduce innovative foundations and hope to inspire future research on the subject. Nowadays, self-organized semiconductor quantum dot (QD) lasers are promising candidates for telecommunication applications [1]. For an introduction to QD-based devices, their growth process, and their optical properties see, for example, [2].

This chapter focuses on the modeling of these QD laser devices and on the discussion of their dynamic properties. Since QD semiconductor materials have a discrete energy sub-bands, one could expect symmetric emission lines, and then the subject of great current interest is a sensitivity of QD semiconductor lasers to optical feedback.

3. Synchronization in chaotic coupled QD lasers

Chaotic synchronization has attracted more interest because of its potential applications in the field of private communication and for the control of chaos in different dynamical systems [1]. Starting in 1990 and following the development of the theory of deterministic chaos synchronization, synchronization was extended to the case of interacting chaotic oscillators [2–5]. Since the definition of chaos involves a quick relationship to decorate the nearby orbits due to their high sensitivity in initial conditions, the synchronization of two associated chaos systems is a fairly intuitive antiretroviral phenomenon. An examination of synchronization phenomena in quantum dot (QD) laser chaotic has been a topic of increasing interest since the past few years [6] because of sensitive to external perturbation as

optical feedback, and these materials have discrete transitions of energy, with expected symmetric emission lines and therefore a low linewidth enhancement factor. This has motivated many studies, with expected benefits including elimination of lasers.

Recently, various methods such as occasional coupling [2, 3], unidirectional coupling [7], and bidirectional coupling [8] with optical feedback [9] have been shown to induce chaos and achieve chaotic synchronization in laser systems. There are different methods for detecting different types of synchronization. Complete synchronization can be identified by drawing a driver component against the responder component while the stage synchronization can be defined by the average frequency [7].

Here, to check for a complete synchronization in both unidirectional and bidirectional, corresponding to this diversity of concepts and complete methods, all the synchronization detection has many different approaches suggested with the aim of quantifying the degree of synchronization between two systems on a continuous scale. These approaches consist of such linear, cross-correlation or time-series tracking as well as nonlinear measures mainly such as bifurcation diagrams.

The remaining chapter is organized as follows: Before we perform any numerical bifurcation studies, we introduce the QD laser model with external optical feedback in Section 2. Section 3 is devoted to the study of the full delay differential equation for the representative value of the frequency of the solitary laser w_o, basic bifurcations of coupling strength in bidirectional synchronization for $k_c \geq 0$ and unidirectional synchronization for $k_c > 0$. Section 4 is devoted to amplitude correlation for two chaotic systems. Finally, we summarize in Section 5.

3.1. Coupling QD laser model

In this section, we consider two semiconductor QD lasers that are delay-coupled to each other with a coupling delay and additionally receive self-feedback with the same delay time τ. The basic coupling scheme is depicted in **Figure 1** (one can see our model with principle translations in Appendix). The coupled system is described by dimensionless rate equations

$$x_1^{\bullet} = x_1(y_1 - 1) + k_{11}\sqrt{x_1 x_{1\tau}}\cos(\phi_1 - \phi_{1\tau} + \Theta) + k_{21}\sqrt{x_2 x_{2\tau}}\cos(\phi_1 - \phi_{2\tau} + \Theta) \quad (1a)$$

$$\Phi_1^{\bullet} = -\frac{\alpha}{2}y_1 - \frac{k_{11}}{2}\sqrt{x_{1\tau}/x_1}\sin(\phi_1 - \phi_{1\tau} + \Theta) - \frac{k_{21}}{2}\sqrt{x_{2\tau}/x_2}\sin(\phi_1 - \phi_{2\tau} + \Theta) \quad (1b)$$

$$x_2^{\bullet} = x_2(y_2 - 1) + k_{22}\sqrt{x_2 x_{2\tau}}\cos(\phi_2 - \phi_{2\tau} + \Theta) + k_{12}\sqrt{x_1 x_{1\tau}}\cos(\phi_2 - \phi_{1\tau} + \Theta) \quad (1c)$$

$$\Phi_2^{\bullet} = -\frac{\alpha}{2}y_2 - \frac{k_{22}}{2}\sqrt{x_{2\tau}/x_2}\sin(\phi_2 - \phi_{2\tau} + \Theta) - \frac{k_{12}}{2}\sqrt{x_{1\tau}/x_1}\sin(\phi_2 - \phi_{1\tau} + \Theta) \quad (1d)$$

where x_k and Φ_k are the normalized photon density and the phase of the kth QD laser, respectively, and α is the linewidth enhancement factor, the phase shift of the light during one round trip in the external cavity ($\tau = 2L/c$) is given by $\Theta = \omega_o\tau$, c is the speed of light. With w_o denoting the frequency of the solitary laser at the lasing threshold. The field labeled by the subscript τ, and k_{ii}, k_{ij} is the feedback and the coupling strength, respectively. The three

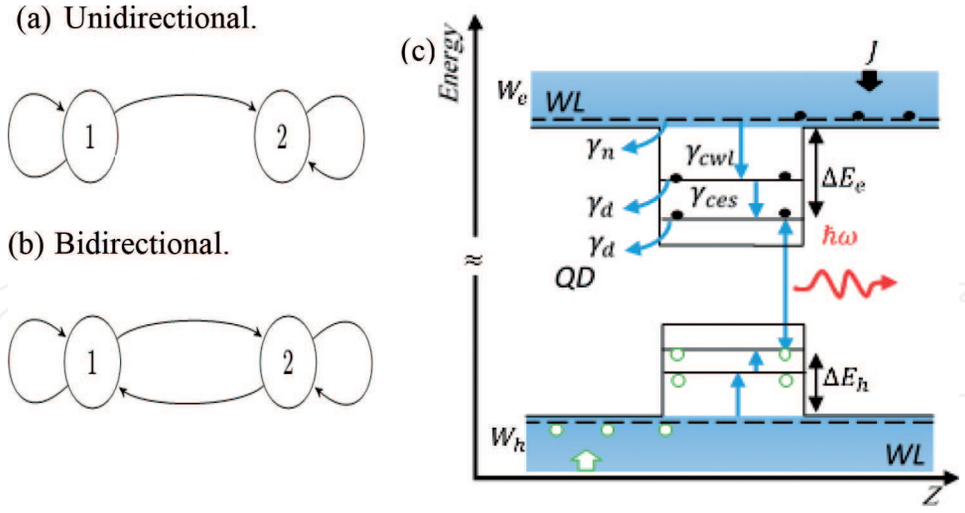

Figure 1. Schematic diagram of two chaotic systems of QD laser with optical feedback object. (a) Unidirectional coupling system. (b) Bidirectional coupling system: (1) transmitter QD laser and (2) receiver QD laser. (c) Schematic energy band diagram of QW and QD. ΔE_e and ΔE_h denote the energy spacing of the QW band edge and the QD ground state (GS) for electrons and holes. $\hbar\omega$ marks the GS lasing energy of the QD.

equations for the occupation probability of a ground and excited states in the QDs (ρ_{gs} and ρ_{es}) and carrier density in the WL (N_{wl}) read:

$$y_k^{\bullet} = \Gamma z_k(\Gamma_1 - y_k) - \Gamma_2 y_k(1 + 2x_k) - \Gamma_1\Gamma_2 \tag{1e}$$

$$z_k^{\bullet} = \Gamma_1 w_k(1 - z_k) - \Gamma_2 z_k - \Gamma z_k(1 - y_k/\Gamma_1)/2 \tag{1f}$$

$$w_k^{\bullet} = \Gamma_3\delta_o - \Gamma_4 w_k - 2\Gamma_3 w_k(1 - z_k) \tag{1g}$$

where the dot denotes derivation with respect to time, δ_o is the bias current (see Appendix for more details). The last terms in (1a)–(1d) are the effect of the chaotic signal. When the chaotic signal from the receiver is zero in the transmitter system, that is, $k_{21} = 0$, the model reduces to the unidirectional system in **Figure 1a**.

3.2. Coupling QD laser results

A QD semiconductor laser display is just one of many examples that interact between many nonlinear similar systems that can lead to a variety of rich emerging behaviors [10]. Neurons, chemical oscillations, or Josephson intersections are other representative cases of nonlinear dynamics that have attracted the attention of researchers from special fields. But, quite astonishingly, only lately has the effects of limited rapid use of signals in the interaction and coupling of several of these systems taken into account.

In this chapter, we accurately focus on the effect of these mismatching strength and delay times, which constitute a rich basis of instabilities, on the dynamics and synchronization of semiconductor QDs laser systems.

In the past work, we emphasized that the QD semiconductors are the ideal candidates for exploring the behavior of nonlinear systems when combined or susceptible to external disturbances [11]. In addition to nonlinear joints in this type of device, it can be well characterized and controlled in experiments, rather than most biologically oriented systems. Besides their inherent nonlinearity, these types of devices can be well characterized and controlled in experiments, as opposed to most of biologically oriented systems. Since then, different configurations of QD semiconductors have been theoretically investigated. The optical interaction of QD-LED has been mostly studied in a single device subject to feedback [12–14].

In a bidirectional optical coupling section, dynamical properties of two semiconductor QD lasers subject to a bidirectional optical coupling are studied. The organization of work in two parts is separated in order to approach separately the cases in which each laser (in addition to the reciprocal function) is subject to self-nourishment or not. First, we start by investigating the coupling of the two chaotic systems in the presence of self-feedback. Unless explicitly mentioned, a symmetric configuration is chosen for the feedback lines ($k_{11} = k_{22}$ and $\tau_1 = \tau_2 \equiv \tau_c$).

Figure 2 shows coupling without self-feedback case, here, we consider the situation in which the self-feedback is zero ($k_{ii} = 0$), and only the mutual coupling excites both lasers simultaneously ($k_{ij} > 0$). This result supports the understanding that threshold decrease in QD semiconductor lasers can just occur during coherent interactions where a superposition of the intra-cavity laser and some injected fields is achievable. In this case, because of the optical interaction is by naturally of phase insensitive, no threshold reduction is expected. Similar to the solitary case, as the strength of feedback is increased, the defeat of stability of the steady state is mediated by a collision in the phase space with the periodic state in a transcritical bifurcation scenario.

In **Figure 2(a)** and **(b)**, we plot a path and indicate the stability of coupling systems as a coupling strength function. **Figure 2** is generated by assuming a small time delay of the coupling so that we promise that no Hopf bifurcation can influence as we will show in the other case. The way to the previous virtual contradiction depends on appreciating that merely at the critical coupling for the system stationary conditions. Eqs. (1a)–(1e) allow for an additional solution consisting of a continuum of steady-states, it is found to connect the two systems at [$w = 0$, $w = \pi$] involved in the stability.

Once the dynamics of our mutually coupled configuration have been characterized in coupling with self-feedback case, we can now approach the different effects and questions raised by the addition of self-feedback to each one of the QD lasers. Thus in the second part of this work, in **Figure 3(a)** and **(b)**, we are investigating the disturbances caused by the delayed reaction between two of the self-oscillation of QD laser. Given the inclusion of feedback loops, we can control the dynamics of the unescorted laser valve between the constant, oscillation, pulsating, and chaotic behavior so that we can investigate the impact of delays on different system synchronization properties. Other dynamic phenomena such as phase synchronization are reviewed.

We now examine the dynamical properties of two semiconductor QD lasers subject to a unidirectional optical coupling. The approach of this cases where two chaotic systems in the

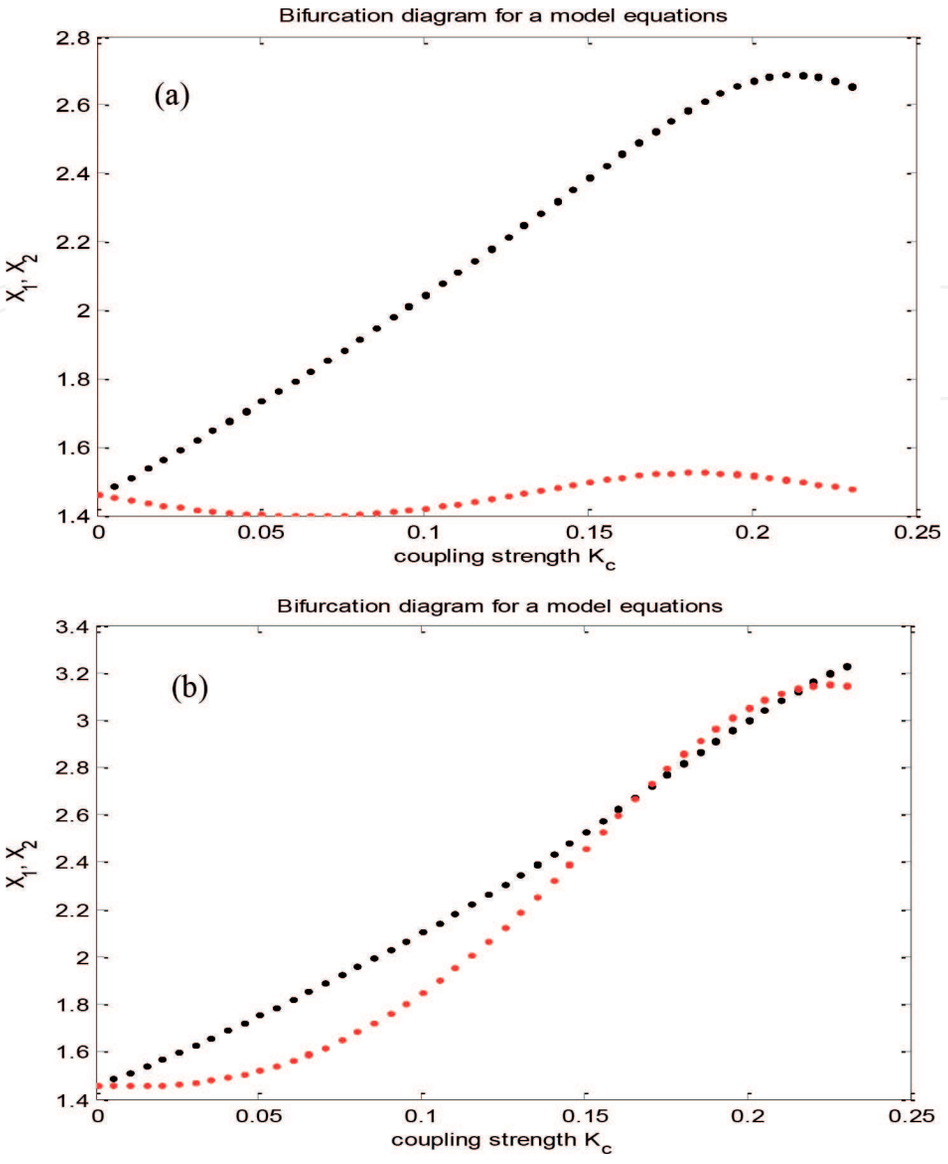

Figure 2. Bifurcation for bidirectional two coupling systems without self-feedback. (a) $w_o = 0$ and (b) $w_o = \pi$. At active delay optical feedback $\tau = 5.7802$, the other conditions are $\delta_o = 0.1$, $k_{ii} = 0$ and $\alpha = 0.9$.

presence of self-feedback ($k_{ii} \neq 0$) and coupling excite lasers ($k_{21} = 0$). **Figure 4(a)** and **(b)** shows the bifurcation diagram for unidirectional two coupling systems with self-feedback objected. In **Figure 4(a)** disynchronization mode appears after a certain value of feedback coupling strength, which suddenly turns into the state of the chaos while the other continues with the steady state. **Figure 4(b)** shows unexpected result when an array of synchronized oscillators becomes desynchronized through the changing of a parameter of the solitary laser. The other parameters are as follows: active delay optical feedback $\tau = 5.7802$, $\delta_o = 0.33$, $k_{ii} = 0.3054$ and $\alpha = 0.9$.

3.3. Different synchronization approaches

In what follows, we pay attention to the investigation on different approaches for achieving synchronization between coupling systems. The synchronization of both lasers is studied here

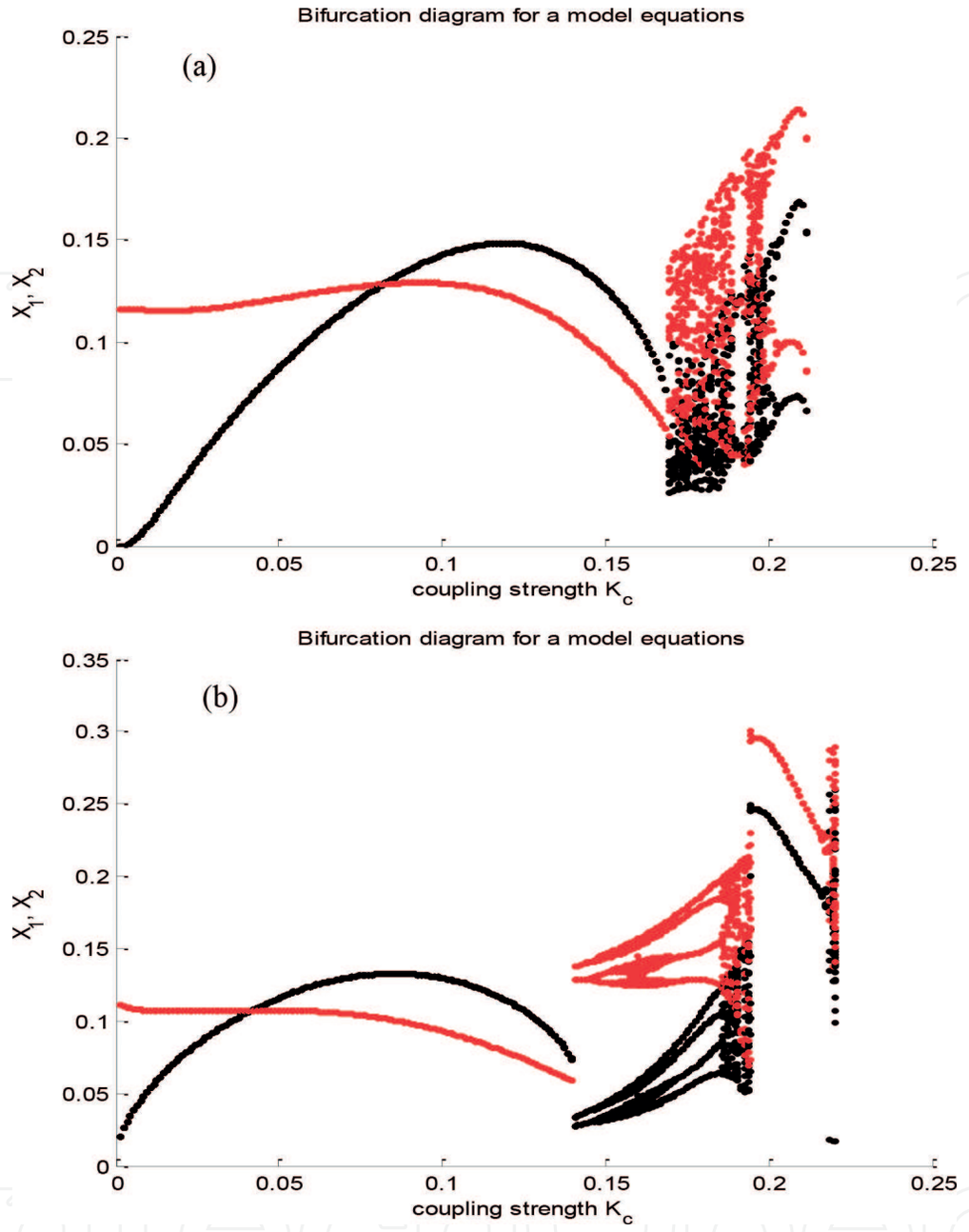

Figure 3. Bifurcation for bidirectional two coupling chaotic systems with self-feedback objected. (a) $w_o = 0$ (b) $w_o = \pi$. At active delay optical feedback $\tau = 5.7802$, the other conditions are $\delta_o = 0.06$, $k_{ii} = 0.258$ and $\alpha = 0.9$.

for three different situations. For identical QD lasers, we first consider the case of bidirectional coupled chaotic oscillators, and secondly, we address the synchronization of unidirectional chaotic oscillators. Finally, we study the unidirectional coupling systems without feedback operation of the receiver laser. The different types of synchronization are characterized by two figures of merit, namely, the correlation degree between amplitudes and the relative time series of the oscillations.

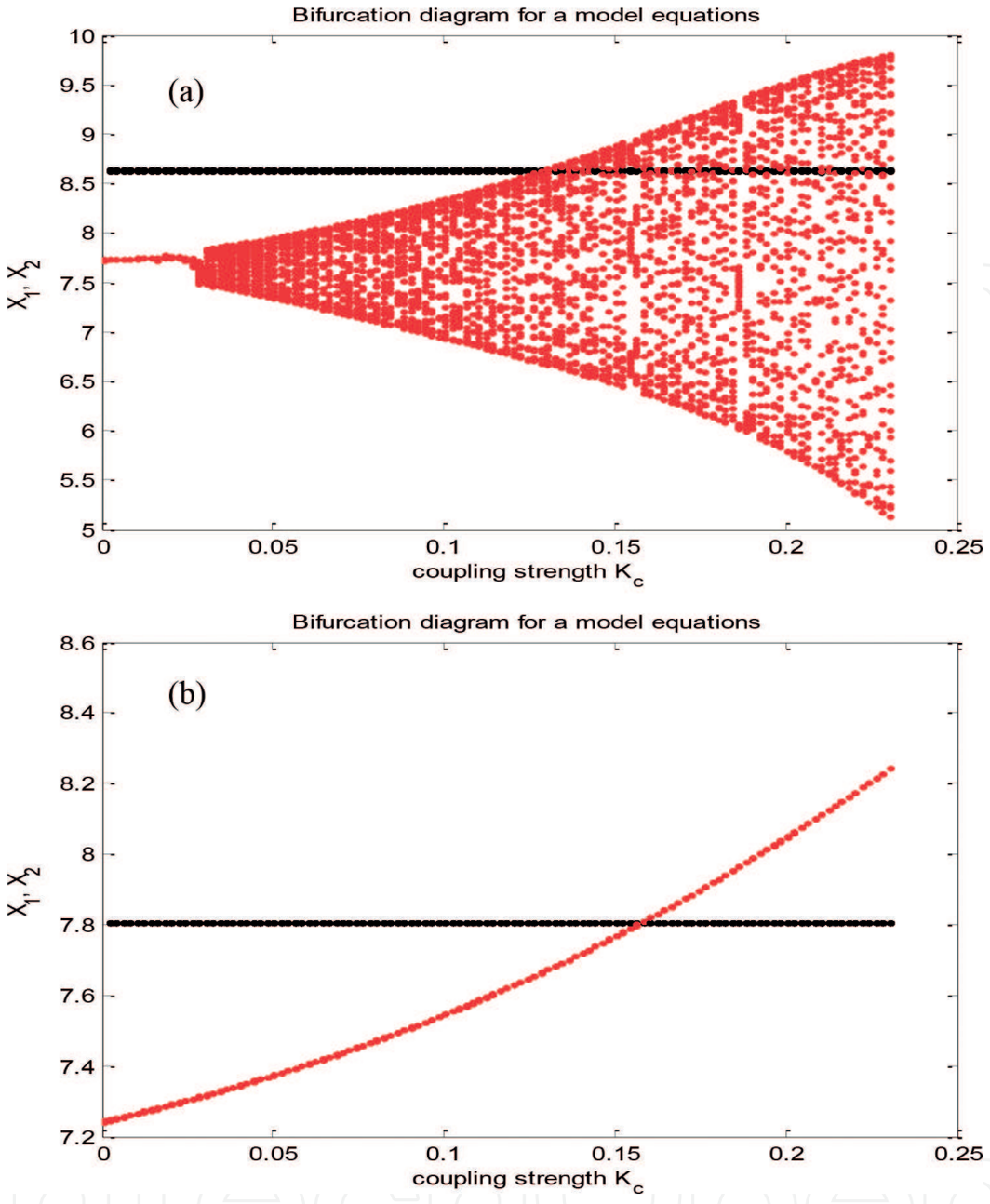

Figure 4. Bifurcation for unidirectional two coupling systems with self-feedback objected. (a) $w_o = 0$ and (b) $w_o = \pi$. At active delay optical feedback $\tau = 5.7802$, the other conditions are $\delta_o = 0.33$, $k_{ii} = 0.3054$, and $\alpha = 0.9$.

Figure 5 shows chaos synchronization in a bidirectional system at conditions $\delta_o = 0.13$, $k_{ii} = 0.25$, $\alpha = 0.9$ and $w = 0$. Output amplitude signal at active delay optical feedback $\tau = 5.7$ of two chaotic systems where output amplitude signal of transmitter (black point-line) and receiver, generalized chaos synchronization at coupling strength ($k_c \geq 0.038$) was shown in **Figure 5(a)**. **Figure 5(b–e)** shows chaotic time series corresponding with (a), which appeared generalized chaos synchronization in **Figure 5(b)**.

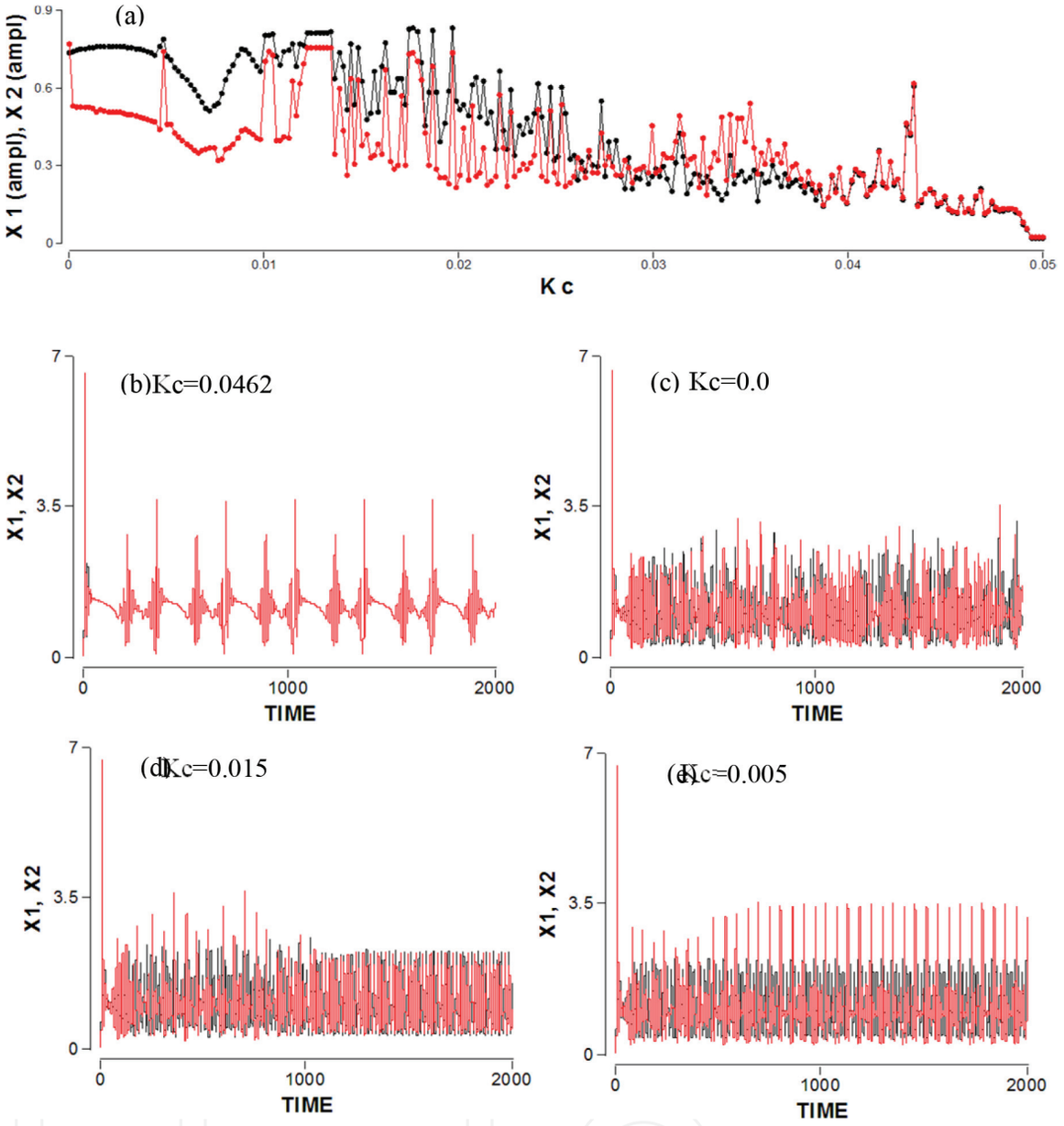

Figure 5. Chaos synchronization in a bidirectional system. (a) Two chaotic systems output amplitude signal, transmitter (black point-line) at active delay optical feedback $\tau = 5.7$ and receiver without feedback (red point-line). (b–e) Chaotic time series corresponding with (a).

Figure 6 shows chaos synchronization in a unidirectional system. **Figure 6(a)** shows generalized chaos synchronization at coupling strength (k_c = 0.01526). **Figure 6(b–e)** shows chaotic time series corresponding with (a), noted that the transmitter behavior is still without change compared with **Figure 6(a)**.

Figure 7 shows unidirectional coupling systems without feedback operation of the receiver laser. Chaos synchronization follows feedback strength of transmitter shown in **Figure 7(a–d)** when coupling strength is projected.

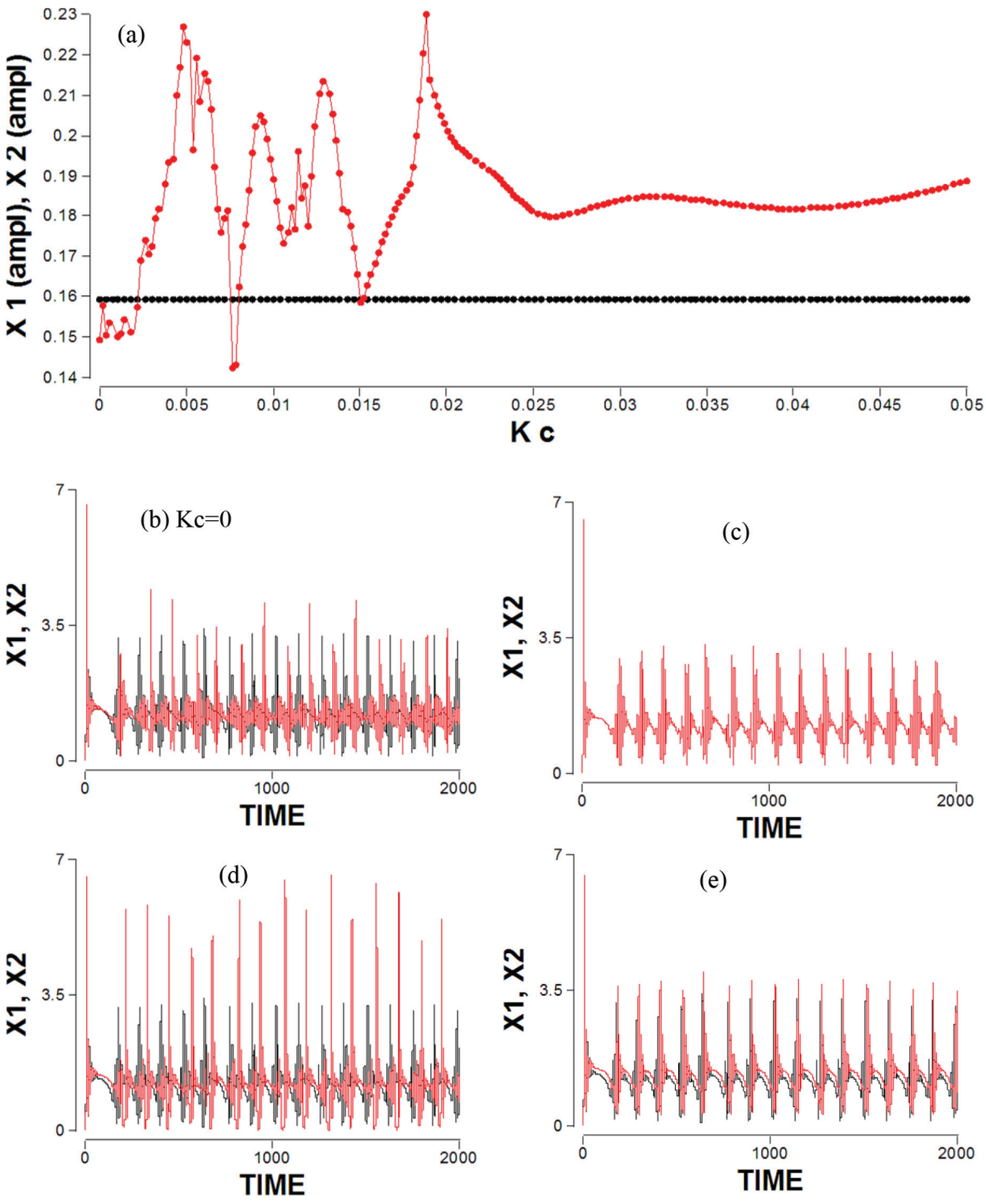

Figure 6. Chaos synchronization in a unidirectional system. (a) Two chaotic systems output amplitude signal, transmitter (black point-line) at active delay optical feedback $\tau = 5.7$ and receiver without feedback (red point-line), generalized chaos synchronization at coupling strength ($k_c = 0.01526$). (b–e) Chaotic time series corresponding with (a). The other conditions are $\delta_o = 0.13$, $k_{ii} = 0.35$, $\alpha = 0.9$, and $w = 0$.

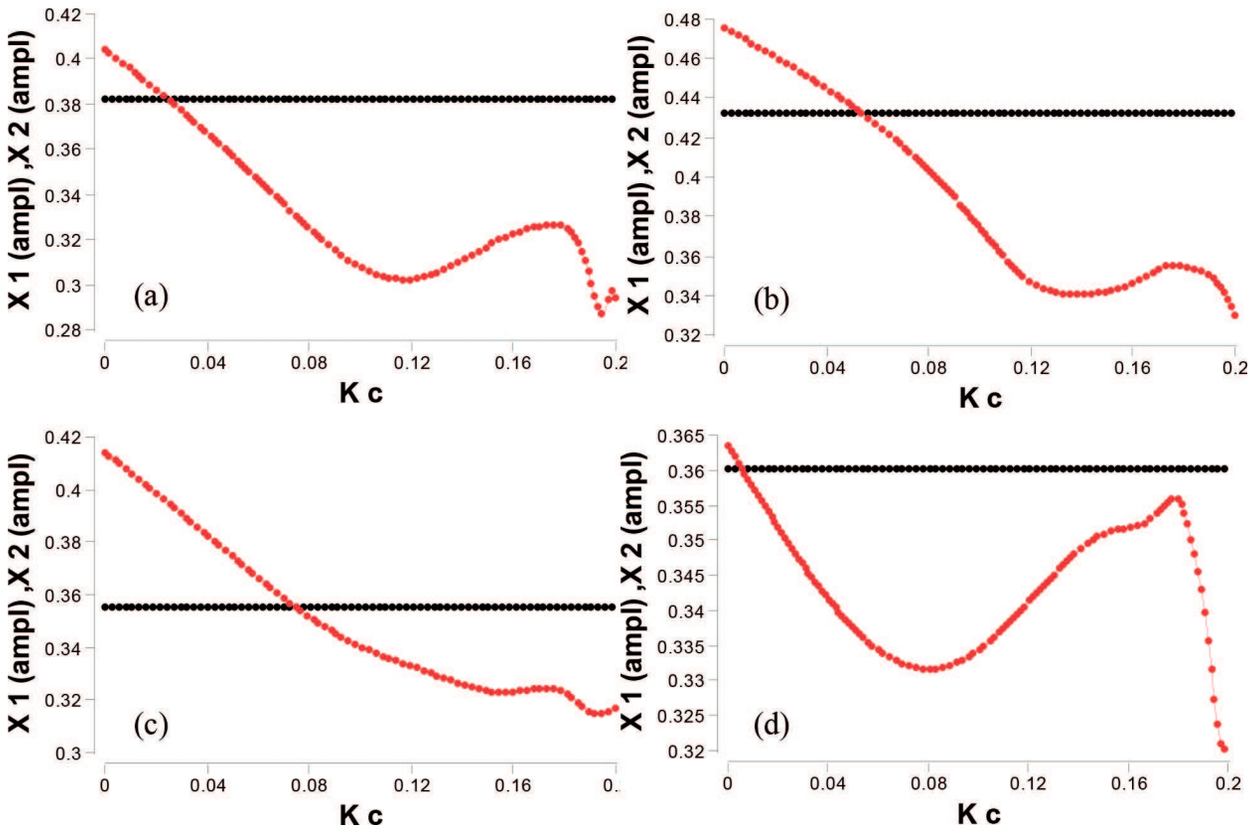

Figure 7. Chaos synchronization in a unidirectional system. Two chaotic systems output amplitude signal, transmitter (black point-line) at active delay optical feedback $\tau = 5.7$ and receiver without feedback (red point-line). Chaos synchronization follows feedback strength when coupling strength is projected. (a) $k_{11} = 0.299$, (b) $k_{11} = 0.3$, (c) $k_{11} = 0.304$, and (d) $k_{11} = 0.3054$. The other conditions are $\delta_o = 0.13$, $\alpha = 0.9$, and $w = 0$.

4. Conclusion

This chapter is concerned with the problem of chaos synchronization estimation in a new semiconductor quantum dot laser dimensionless model. The need to know effect of parameters in our model with coupling case at different approach of chaos synchronization occurs throughout the development of bifurcation diagrams, which reduced dynamics of model. The approach presented here builds on the existing work that uses synchronization as a tool for parameter estimation. Some important issues of chaos synchronization are addressed in this chapter. The central issue is the choice of coupling strength between the systems, which is considered through bifurcations depending on coupling kind.

A. Appendix

The field equation is defined as a complex stochastic differential equation. The aim is to transform the complex stochastic differential equation form field equation (E) into two real stochastic

differential equations for the photon density $S = |E|^2$ and the phase Φ. This is just a transformation to polar coordinates without the stochastic term [14]. Averaging over the stochastic terms, the final rate equations for the photon density S, the phase of the electric field Φ, and the three equations for the occupation probability of a ground and exited states in the QDs (ρ_{gs} and ρ_{es}) and carrier density in the WL (N_{wl}) read:

$$S^{\bullet} = \left[v g_o \left(2\rho_{gs} - 1 \right) - \gamma_s \right] S + \gamma \sqrt{S S_\tau} \cos\left(\phi - \phi_\tau \right) \tag{2a}$$

$$\phi^{\bullet} = -\frac{\alpha}{2} v g_o \left(2\rho_{gs} - 1 \right) - \frac{\gamma}{2} \sqrt{S_\tau / S} \sin\left(\phi - \phi_\tau \right) \tag{2b}$$

$$\rho_{gs}^{\bullet} = \gamma_{c_{es}} \rho_{es} \left(1 - \rho_{gs} \right) - \gamma_d \rho_{gs} - g_o \left(2\rho_{gs} - 1 \right) S \tag{2c}$$

$$\rho_{es}^{\bullet} = \gamma_{c_{wl}} N_{wl} \left(1 - \rho_{es} \right) - \gamma_d \rho_{es} - \gamma_{c_{es}} \rho_{es} \left(1 - \rho_{gs} \right) \tag{2d}$$

$$N_{wl}^{\bullet} = \frac{J}{e} - \gamma_n N_{wl} - 2\gamma_{c_{wl}} N_{wl} \left(1 - \rho_{es} \right) \tag{2e}$$

In our approach, the carrier-light interaction is summarized in the photon density S, which includes all longitudinal modes. The factor 2 in Eq. (2e) accounts for the twofold spin degeneracy in the quantum dot energy levels. A similar factor 2 is included in the definition of the differential gain factor g in Eq. (2a) [11]. For numerical purposes, it is useful to rewrite Eqs. (2) in a dimensionless form. To this end, we introduce the new variables

$x = \frac{g_o}{\gamma_d} S,\ \Phi \equiv \Phi,\ y = \frac{g_o v}{\gamma_s} \left(2\rho_{gs} - 1 \right),\ z \equiv \rho_{es},\ w = \frac{\gamma_{c_{wl}}}{g_o v} N_{wl},\ \Gamma = \frac{\gamma_{c_{es}}}{\gamma_s},\ \Gamma_1 = \frac{g_o v}{\gamma_s},\ \Gamma_2 = \frac{\gamma_d}{\gamma_s},.$

$\Gamma_3 = \frac{\gamma_{c_{wl}}}{\gamma_s},\ \Gamma_4 = \frac{\gamma_n}{\gamma_s},\ \delta_o = \frac{J}{g_o v q}$ and the time scale $t' = \gamma_s t$. The rate

$$x^{\bullet} = x(y-1) + \varepsilon \sqrt{x x_\tau} \cos\left(\phi - \phi_\tau \right) \tag{3a}$$

$$\Phi^{\bullet} = -\frac{\alpha}{2} y - \frac{\varepsilon}{2} \sqrt{x_\tau / x} \sin\left(\phi - \phi_\tau \right) \tag{3b}$$

$$y^{\bullet} = \Gamma z (\Gamma_1 - y) - \Gamma_2 y (1 + 2x) - \Gamma_1 \Gamma_2 \tag{3c}$$

$$z^{\bullet} = \Gamma_1 w (1 - z) - \Gamma_2 z - \Gamma z (1 - y/\Gamma_1)/2 \tag{3d}$$

$$w^{\bullet} = \Gamma_3 \delta_o - \Gamma_4 w - 2\Gamma_3 w (1 - z) \tag{3e}$$

where $\varepsilon = \gamma / \gamma_s$. The well-established assumptions here are that the delay time τ is larger than the laser roundtrip time inside the active region (**Figure 1**).

Author details

Hussein B. Al Husseini[1] and Kais A.M. Al Naimee[2,3]*

*Address all correspondence to: kais.al-naimee@ino.it

1 Nassiriya Nanotechnology Research Laboratory (NNRL), Science College, Thi-Qar University, Nassiriya, Iraq

2 Department of Physics, College of Science, University of Baghdad, Baghdad, Iraq

3 Istituto Nazionale di Ottica—CNR Firenze, Italy

References

[1] Ohtsubo J. Chaotic dynamics in semiconductor lasers with optical feedback. In: Wolf E. editor. Progress in Optics. Vol. 44. Amsterdam: North-Holland; 2002. p. 25. Chap. 1

[2] Usman M. Multi-million atom electronic structure calculations for quantum dots [PhD thesis]. Purdue University; 2011

[3] Al-Khursan AH. Intensity noise characteristics in quantum-dot lasers: Four-level rate equations analysis. Journal of Luminescence. 2005;**113**:129-136

[4] Sprott JC. Chaos and Time–Series Analysis. Oxford; 2003

[5] Al Khursan AH, Ghalib BA, Al Obaidi SJ. Numerical simulation of optical feedback on a quantum dot lasers. Physics of Semiconductor Devices. 2012;**46**(2):213-220. ISSN: 1063-7826

[6] Pikovsky AS, Rosenblum MG, Kurths J. Synchronization. A Universal Concept in Nonlinear Sciences. Cambridge, UK: Cambridge University Press; 2001

[7] Ghalib BA, Al-Obaidi SJ, Al-Khursan AH. Quantum dot semiconductor laser with opto-electronic feedback. Superlattices and Microstructures. 2012;**52**:977-986

[8] Ananthakrishna G, Bharathi MS. Dynamical approach to the spatiotemporal aspects of the portevin - le chatelier effect: Chaos, turbulence, and band propagation. Physical Review E. 2004;**70**:026111

[9] Al Naimee K, Al Husseini H, Abdalah SF, Al Khursan A, Khedir AH, Meucci R, Arecchi FT. Complex dynamics in quantum dot light emitting diodes. European Physical Journal D. 2015;**69**(257):1-5

[10] Voss HU, Timmer J, Kurths J. Nonlinear dynamical system identification from uncertain and indirect measurements. International Journal of Bifurcation and Chaos. 2004;**14**:1905-1933

[11] Al Husseini HB. Control of nonlinear dynamics of quantum dot laser with external optical feedback. Journal of Nanotechnology in Diagnosis and Treatment. 2016;**4**:5-14

[12] Al Husseini HB, Al Naimee KA, Al-Khursan AH, Khedir AH. External modes in quantum dot light emitting diode with filtered optical feedback. Journal of Applied Physics. 2016;**119**:224301. DOI: 10.1063/1.4953651

[13] Huyet G, O'Brien D, Hegarty SP, McInerney JG, Uskov AV, Bimberg D, Ribbat C, Ustinov VM, Zhukov AE, Mikhrin SS, Kovsh AR, White JK, Hinzer K, Spring Thorpe AJ. Quantum dot semiconductor lasers with optical feedback. Physica Status Solidi (b). 2004;**201**:345-352

[14] Fu Y, Jiang G. Chaos and chaos synchronization of semiconductor lasers with optoelectronic feedback and bidirectional couplings. Journal of Optoelectronics and Advanced Materials. 2010;**12**(6):1350-1355

IntechOpen